



Functional characterization of edible films based on reactive extrusion acetylated corn starch

Ernesto Aguilar-Palazuelos¹ · Perla Rosa Fitch-Vargas² · Luis Fernando Pérez-Vega¹ · Irma Leticia Camacho-Hernández¹ · José de Jesús Zazueta-Morales¹ · Abraham Calderón-Castro¹

Received: 20 September 2022 / Accepted: 23 December 2022

© The Author(s), under exclusive licence to Springer Science+Business Media, LLC, part of Springer Nature 2023

Abstract

There is great interest in developing edible films (EFs) with functional properties made from renewable resources to solve environmental problems associated with plastic waste and improve food preservation and safety. Corn starch is the main raw material employed for producing EFs due to its biodegradability, and availability. Nonetheless, the hydrogen bonding interactions of the native starch structure are strong, limiting its use in the development of bioplastics. In addition, starch-based materials are hydrophilic and lack mechanical integrity. A measure to overcome these disadvantages is the starch native structure modification by a reactive extrusion, where acetylation is one of the most applied chemical modifications. The functionality of acetylated modified corn starch is determined by the degree of substitution (DS). Glycerol is a widely used plasticizer in the food area and is essential in forming starch-based EFs, improving their flexibility and elongation. Hence, this research aimed to develop acetylated modified corn starch edible films (AcEFs) with a DS (0–0.2) and Glycerol Content (GC) (15–30%) to improve its functional properties. The acetylated modified corn starch was obtained by reactive extrusion. The casting technique was used to obtain AcEFs; these were characterized and optimized, evaluating the deformation, puncture resistance, carbon dioxide permeability, water vapor permeability, and water solubility. The data was analyzed using the surface response methodology, and the optimization was carried out using the numerical method. According to the optimization study, the AcEFs with the best mechanical and barrier properties were obtained with 0.16 DS and 18.30% GC.

Keywords Modified corn starch · Reactive extrusion · Acetylated modified corn starch edible films · Acetylation · Glycerol content

✉ Abraham Calderón-Castro
abcalcas@uas.edu.mx

Ernesto Aguilar-Palazuelos
eaguilar@uas.edu.mx

Perla Rosa Fitch-Vargas
perlafitch@uas.edu.mx

Luis Fernando Pérez-Vega
luis.pv95@gmail.com

Irma Leticia Camacho-Hernández
lcamacho@uas.edu.mx

José de Jesús Zazueta-Morales
zazuetaj@uas.edu.mx

¹ Facultad de Ciencias Químico-Biológicas, Universidad Autónoma de Sinaloa. Ciudad Universitaria. Culiacán, 80013 Culiacán, Sinaloa, Mexico

² Facultad de Ciencias del Mar, Universidad Autónoma de Sinaloa, Paseo Claussen S/N, Col. Los Pinos, 82000 Mazatlán, Sinaloa, Mexico

Introduction

In recent years, Edible Films (EFs) have received much interest as a technique to extend the shelf life of vegetables and fruits. The EFs are pre-formed thin layers produced by edible materials, molded into solid plates, and placed on the food product's surface. The materials used in EFs must be safe for human consumption. Moreover, the EFs design is crucial in food preservation because it determines the film's functionality, including moisture transfer regulation, selective gas barrier, and mechanical properties improvement. These functional characteristics determine the EFs' efficacy. In addition, it is essential to study the mechanical and barrier characteristics of EFs since they impact product efficacy during transport and storage [1–3].

Native corn starch has been a commonly used ingredient for producing EFs [4–6]. This biopolymer is an available, sustainable, low-cost resource that can create a

continuous matrix with low permeability to oxygen. Nevertheless, starch EFs have significant drawbacks, including low mechanical strength, brittleness, and high solubility, limiting their application in food packing [7, 8]. The use of modified starch as a film-forming matrix offers a solution to these limitations [9, 10].

Chemical modification of the native starch structure could be a helpful tool for improving the functional characteristics of EFs. The starch modification improves the thermoplastic processability and hydrophobicity of EFs [11]. The food industry's most common starch chemical modifications are hydrolysis, oxidation, cross-linking, and substitution by esterification with acetic anhydrides. The modification by acetylation can reduce the water affinity of processed starch, replacing the three free hydroxyl groups on C₂, C₃, and C₆ with hydrophobic acetyl groups. The chemical properties of acetylated starch depend on the reaction conditions, starch source, and degree of substitution (DS). FDA approves acetylated starch with DS of 0.2 for food and drug applications [12, 13].

The extruders can produce modified starches in a continuous process. The reactive extrusion is based on high temperatures for short periods and is an affluent-free, ecologically friendly, and energy-efficient alternative [14]. In this method, the starch biopolymer is heated, transported, and mixed by a single or twin screw, which is then forced against a die at high pressure and temperature, producing molecular changes [11, 15]. Starch exhibits thermoplastic properties when the action of heat and shear disintegrates it in the presence of plasticizers. Thermoplastic starch has certain disadvantages, such as poor mechanical properties and high sensitivity to water. Hence, to overcome these drawbacks, an additional chemical modification is usually necessary [2, 6]. In previous research, Calderon-Castro et al. [16] designed a mathematical model to predict the conditions of the reactive extrusion process for the production of acetylated modified corn starch with different safe-food-use DS (0–0.2) and water resistance, using as study factors extrusion temperature (80–160 °C), Screw Speed (100–200 rpm), and acetic anhydride content (0–13%).

On the other hand, due to the strong intramolecular hydrogen bonding along starch chains, the production of bioplastics is complex. Consequently, the plasticizer is an additive that can improve starch-based films' flexibility, elongation, and toughness. The main purpose of plasticizers is to break the starch granules, diminishing the intermolecular bonding interaction. The plasticizer molecules can disturb the interaction in a polymeric matrix by acting as a lubricant. One of the plasticizers that are widely used is water. However, films containing only water are brittle. The commonly used plasticizers are polyols (glycerol, sorbitol, among others) and low molecular weight sugars

Table 1 Conditions to obtain the DS of the acetylated modified corn starch using the reactive extrusion

DS	Prediction conditions		
	ET (°C)	SS (rpm)	Acetic anhydride (%)
0	160	100	0
0.03	160	100	1.49
0.10	160	100	4.85
0.17	160	200	5.88
0.20	80	100	7.88

DS Degree of substitution, ET Extrusion temperature, SS Screw speed

(sucrose, glucose, xylose, fructose, among others), where glycerol is the most employed [2, 4, 6].

Starch-based EFs can be employed as food packaging due to their flexibility and resistance to rupture, avoiding possible deformations, protecting from damage, and facilitating handling. In addition, EFs with low gas permeability could control the gas exchange between food and the environment, improving food preservation. While water solubility is an essential property of starch-based EFs, indicating their integrity in an aqueous medium and possibly the protective characteristics for fresh and frozen foods with high water activity [2, 3]. Many research works have studied the physicochemical characterization of EFs based on native and modified starch [4, 5, 9, 17–20]. Nonetheless, there are few reports on the study of the effect of the safe-food-use DS on the functional characteristics of acetylated modified corn starch EFs. Therefore, this study aims to develop EFs based on acetylated modified corn starch with safe-food-use DS and GC to improve their mechanical and barrier properties.

Materials and methods

Raw materials

Native corn starch (*Zea mays* L.) (Ingredient, Jalisco, Mexico) was employed for starch modification. The acetylated modified corn starch was obtained by employing acetic anhydride (JT Baker, Pennsylvania, USA). Glycerol (JT Baker®, Center Valley, USA) was used as a plasticizer.

Starch chemical modifications by reactive extrusion process

Acetylated modified corn starch with safe-food-use DS was obtained according to Calderón-Castro et al. [16]. A twin-screw extruder (Model LT32L, Shandong Light M&E, China) with a 20:1 L/D ratio, circular die with a diameter of

4 mm, and compression 2:1 was employed. Table 1 shows the conditions for getting the acetylated modified corn starch with different safe-food-use DS using the reactive extrusion process. Extruded samples were ground using a hammer mill (Pulvex model 200, Mexico City, Mexico), sieved in a mesh of 200 μm particle size, and dried in an oven (Yamato DKN402C, CA, USA) at 60 °C for 12 h. The slurry was centrifuged at 6000 rpm for 10 min to increase pH to 5.0. The pellet was then washed and dried for 24 h at 45 °C. The dried powder was ground and put through a sieve with a mesh opening of 200 μm . For further analysis, MS were packaged in polyethylene bags and kept at a temperature of 25 °C and relative humidity of 53%.

Acetylated starch edible films preparation

The casting technique was used to obtain acetylated modified corn starch edible films (AcEFs) [2]. The safe-food-use degree substitution (DS) and Glycerol Content (GC) for producing AcEFs are shown in Table 2. A formulation with a ratio of 10:1 (water: modified corn starch-GC) was employed. The solution was heated for 10 min on a plate at 80 °C (Fisher Scientific, Waltham, MA, USA). Then, 25 mL of the gelatinized mixture was poured into acrylic molds and dried at 60 °C for 2 h to obtain the AcEFs (Yamato DKN402C, CA, USA). The thickness of the AcEFs was obtained using a digital micrometer (Digital Insize, Model 3109-25 A, Spain), recording values of $50 \pm 5 \mu\text{m}$. Finally, the films were stored in a container with a saturated solution

Table 2 Experimental design for the elaboration EFs based on acetylated modified corn starch

Assay ^a	Independent variables			
	Codified		Decodified	
	X ₁	X ₂	DS	GC (%)
1	-1.000	-1.000	0.03	17.20
2	1.000	-1.000	0.17	17.20
3	-1.000	1.000	0.03	27.80
4	1.000	1.000	0.17	27.80
5	-1.414	0.000	0.00	22.50
6	1.414	0.000	0.20	22.50
7	0.000	-1.414	0.10	15.00
8	0.000	1.414	0.10	30.00
9	0.000	0.000	0.10	22.50
10	0.000	0.000	0.10	22.50
11	0.000	0.000	0.10	22.50
12	0.000	0.000	0.10	22.50
13	0.000	0.000	0.10	22.50

X₁ = DS = Degree of substitution, X₂ = GC = Glycerol content

^aStandard order

of Mg(NO₃)₂·6H₂O (JT Baker®, Center Valley, USA), producing a relative humidity of 53%.

Mechanical properties

The most cited characteristics to describe the mechanical properties of the EFs are Deformation (D) and Puncture Strength (PS). Puncture tests with a texture analyzer (INSTRON 3342, Norwood, MA, USA) were adapted to determine the D and PS of AcEFs [2]. Mechanical properties were measured using twenty EFs samples from each treatment. Each sample had a diameter of 50 mm and was mounted on a texturometer plate with a hole of 30 mm. With a constant speed of 1 mm s⁻¹, a cylindrical probe of 10 mm in diameter was moved perpendicular to the surface of AcEFs. The cutting distance from the sample contact until its break (D), in millimeters (mm), and the maximum force before the break (PS), in Newtons (N), were measured.

Barrier properties

Carbon dioxide permeability (CO₂P)

The CO₂P was measured using the methodology reported by Ayranci et al. [21]. Firstly, 4 g of ascarite and 4 g of calcium chloride (CaCl₂) were put into acrylic containers. The AcEFs were fixed with parafilm at the top of the containers. The sealed containers were weighed and placed into a desiccator with a CO₂ atmosphere and constant pressure (101324.71 Pa). Ascarite absorbed CO₂ and produced water as a result of a chemical reaction. The water was held by anhydrous CaCl₂. The weight increment of the acrylic containers was measured every two h for two days. A slope was calculated by plotting the data as a function of time. The CO₂ transmission (CO₂T) was calculated by dividing the slope value by the film's total area exposed to the transmission. Equation (1) was employed to calculate CO₂P:

$$CO_2P = \frac{CO_2T}{p} \times l \quad (1)$$

where p (101324.71 Pa) is the pressure within the desiccator and l is the thickness of EFs.

Water vapor permeability (WVP)

The WVP of AcEFs was measured according to Fitch-Vargas et al. [2]. The AcEFs were fixed on glass containers with 15 g of anhydrous calcium chloride (CaCl₂). Subsequently, the containers were put in a desiccator with a saturated sodium chloride solution to obtain 75% relative humidity

at 25 ± 1 °C. The weight of anhydrous CaCl_2 in a glass container was measured every 12 h for 4 days. For each treatment, five measurements were obtained. The following Eq. (2) was used to determine WVP:

$$WVP = \frac{Mm \times E}{A \times t \times \Delta p} \quad (2)$$

where Mm = absorbed moisture mass (g), E = EFs thickness (m), t = time (s), A = exposed area (m^2), and Δp = partial pressure differential through the EFs (Pa).

Water solubility (S)

The S was calculated as a disintegrated material percentage using the method provided by Chiumarelli and Hubinger [22]. For each treatment, five measurements were obtained. Equation (3) was used to calculate the WS:

$$S = \frac{(w_i - w_f)}{w_i} \times 100 \quad (3)$$

where w_i = initial sample weight, and w_f = final sample weight.

Experimental design

A central composite rotatable model with $\alpha = 1.414$ was used to optimize the two independent variables: safe-food-use degree of substitution (DS, 0–0.2) and Glycerol Content (GC, 15–30%) (Table 2), to obtain AcEFs with the highest D and PS values and lowest CO_2P , WVP, and S values. The GC levels used were selected based on preliminary experiments and the technical limitations of the study. Three main steps are involved in optimization using the RSM method: first, statistically designed experiments; second, estimating the coefficients in a mathematical model; and third, predicting the response and evaluating the model's suitability for the experiment setup. Each numeric factor is varied over five levels. Plus and minus alpha (axial points), plus and minus 1 (factorial points), and the center points. In the factorial design, thirteen experiments were included. The factorial design included four data points (extremes) at levels (–1) and (+1), four axial points outside of the factorial matrix but inside the experimental domain, which corresponded to the values –1.414 and +1.414, and a third set composed of five replicates of the points at the origin of the reference system (central-points), coded as (0, 0). The assays

were performed randomly (Table 2). The significance of the factors model was evaluated by analysis of variance (ANOVA) (P value and F-value at 95% confidence level). The data analysis of the experimental design and the response surface graphs were carried out using the Response Surface Methodology (RSM) with the Design Expert® Software Version 8 package (Stat-Ease, Inc., Minneapolis., USA). Equation 4 shows the second-order polynomial model used to predict the behavior of the response variables:

$$y_i = b_0 + b_1x_1 + b_2x_2 + b_1^2x_1^2 + b_2^2x_2^2 + b_1b_2x_1x_2 \quad (4)$$

where y_i = dependent variable; b_i = regression model coefficients; x_1 = degree of substitution (DS), and x_2 = Glycerol Content (GC). The numerical optimization technique of the RSM was used. In this optimization, it was selected the desired goals, known as constraints for each response and factors with their weight and importance. The step-wise regression model was developed for process variable optimization with high desirability. In addition, triplicate experiments were performed to validate the optimized conditions. Statgraphics plus 6.0 software was used to verify the existence of significant differences between the predicted and experimental values of each response variable using Fisher's Least Significant Difference (LSD) test ($P > 0.05$). The optimum AcEFs were characterized according to their microstructural properties (XRD and FT-IR).

X-ray diffraction (XRD)

Native corn starch and acetylated modified corn starch at a particle size < 200 μm and AcEFs samples were packed into glass containers and put into an X-ray diffractometer (Rigaku Model Last D/Max-2100 Rigaku Denki Co. Ltd., Japan). Diffractograms were obtained by employing a 5–30° Bragg sweep angle over a scale of 2θ with 0.02 intervals. The relative crystallinity was measured by differentiating the crystalline and amorphous zones in diffractograms [16].

Infrared spectroscopy analysis (FT-IR)

Infrared spectroscopy was used to record the FT-IR patterns (Nicolet™ iS™ 50, Thermo Fisher Scientific Co., Waltham, MA, U.S.A.). The FT-IR spectra of 4000–300 cm^{-1} were obtained at a scan rate of 32 and resolution of 4 cm^{-1} [16].

Results and discussion

Functional characterization of acetylated starch edible films (AcEFs)

Deformation (D)

Table 3 shows the statistical analysis for deformation (D), recording a significant regression model ($R^2_{adj} = 0.80$, coefficient of variation (CV) = 12.82%, standard deviation (SD) = 1.04 mm, P of $F < 0.01$) without lack of fit ($P = 0.1320$). There is a 13.00% chance that a “Lack of Fit F-value” this large could occur due to noise.

Non-significant lack of fit is good, so the model fits. Values of “ $Prob > F$ ” less than 0.05 indicate that model terms are significant. DS and GC were significant model terms ($P < 0.05$). The DS’s linear term, with a percentage of 27.52%, significantly affected the D, decreasing its values with the increase of the DS. On the other hand, the linear term of GC had the most significant impact (72.48%) in D, increasing its values with the increase of GC. The prediction model obtained for D is shown in Eq. (5):

$$D = +12.32 - 1.26DS + 3.32GC \quad (5)$$

The D values are shown in Table 4, recording a range of 6.57–16.04 mm. Starch-based EFs have limited flexibility or deformation compared to synthetic materials. Several

Table 3 Regression coefficients and ANOVA for the D, PS, CO₂P, WVP, and S responses variable in the AcEFs

	D	PS	CO ₂ P	WVP	S
Intercept	+ 12.32	+ 13.77	-2.43×10^{-13}	$+3.15 \times 10^{-11}$	+ 25.63
DS	-1.26 (0.0472)*	+2.14 (<0.01)	-8.47×10^{-12} (<0.01)	-3.69×10^{-12} (<0.01)	- 5.09 (<0.01)
GC	+3.32(<0.01)	-3.64(<0.01)	$+9.20 \times 10^{-14}$ (<0.01)	-7.08×10^{-12} (<0.01)	+2.87(<0.01)
R ² adjusted	0.80	0.80	0.93	0.82	0.89
CV (%)	12.82	12.22	17.23	9.49	5.75
SD (units)	1.04	1.68	1.63×10^{-14}	2.98×10^{-12}	1.94
F value	26.95	25.37	83.78	28.70	36.40
P of F (model)	<0.01	<0.01	<0.01	<0.01	<0.01
Lack of fit	0.13	0.07	0.28	0.09	0.86

D Deformation, PS Puncture Strength, CO₂P Carbon Dioxide Permeability, WVP Water Vapor Permeability, S Water Solubility, DS Degree of Substitution, GC Glycerol Content, NS Non-significative, $\alpha < 0.05$, CV Coefficient of variation, SD Standard deviation

*P of F

Table 4 Design and experimental results of the response variables evaluated to AcEFs

Treatment ^a	Independent variables		Dependent variables				
	DS	GC (%)	D (mm)	PS (N)	CO ₂ P (mL m/s m ² pa)	WVP (g m/s m ² pa)	S (%)
1	0.03	17.20	8.50	14.68	1.10×10^{-12}	2.57×10^{-11}	28.57
2	0.17	17.20	6.63	18.66	8.97×10^{-14}	2.25×10^{-11}	20.98
3	0.03	27.80	15.08	10.40	1.84×10^{-12}	4.01×10^{-11}	33.48
4	0.17	27.80	13.18	12.07	8.00×10^{-13}	3.23×10^{-11}	26.86
5	0.00	22.50	15.35	8.97	2.04×10^{-12}	4.16×10^{-11}	36.62
6	0.20	22.50	10.88	17.28	9.82×10^{-14}	2.84×10^{-11}	17.90
7	0.10	15.00	6.57	22.30	1.46×10^{-13}	2.25×10^{-11}	21.04
8	0.10	30.00	16.04	9.42	1.88×10^{-12}	4.55×10^{-11}	29.67
9	0.10	22.50	12.86	12.80	1.19×10^{-12}	2.98×10^{-11}	26.72
10	0.10	22.50	13.25	12.15	9.17×10^{-13}	2.72×10^{-11}	23.49
11	0.10	22.50	12.83	12.32	8.92×10^{-13}	3.11×10^{-11}	26.86
12	0.10	22.50	15.30	13.73	8.56×10^{-13}	3.16×10^{-11}	26.73
13	0.10	22.50	13.67	14.18	8.91×10^{-13}	3.03×10^{-11}	25.34

DS Degree of substitution, GC Glycerol content, D Deformation, PS Puncture strength, CO₂P Carbon dioxide permeability, WVP Water vapor permeability, S Water solubility

^aStandard order

authors have reported lower D values than those obtained in this study. Maran et al. [7] produced tapioca starch-based EFs, evaluating the concentration of starch (1–3 g), glycerol (0.5–1.0 mL), and agar (0.5–1.0 g), reporting D values of 3.48–4.72 mm. Mali et al. [23] in EFs based on yam starch recorded puncture D values from 3 to 5 mm.

The DS and GC behavior on the D of AcEFs is shown in Fig. 1a. The highest value of D was 16.04 ± 1.76 mm, and it was obtained at 30% of GC and 0.1 of DS. Due to the increasing GC, the increase in D could be attributed to a reduction in intermolecular interactions among polymeric chains, favoring the molecule's mobility [18]. Furthermore, increasing GC could increase the AcEFs moisture content, reducing the force between adjacent molecules [24]. On the other hand, the DS slightly reduces the D of the AcEFs. It could be attributed to the strong molecular interactions of the modified starch resulting from the increase in DS during acetylation, causing greater rigidity in the EFs [6, 10]. Likewise, the starch acetylation produces partial hydrolysis that reduces the length of the glucose chains, decreasing the D of the EFs [20].

Puncture strength (PS)

The puncture strength (PS) represents the maximum force to break a material. With an $R^2_{adj} = 0.83$, $CV = 12.22\%$, $SD = 1.68$ N, P of $F < 0.01$, and no lack of fit (P of $F > 0.05$), PS demonstrated a significant model of regression (Table 3). The Model F-value of 25.37 implies that the model is significant. There is only a 0.01% chance that a “Model F-value” this large could occur due to noise. The PS was significantly affected by the DS and GC linear terms ($P < 0.01$). The linear term of the DS had a positive impact of 37.02% on the PS; it increased its values. Otherwise, the GC, although it had an impact of 62.98% on the response variable, had a negative impact, decreasing the PS values. The mathematical model for PS is shown in Eq. (6):

$$PS = + 13.77 + 2.14 DS - 3.64 GC \quad (6)$$

The EFs used as food packaging require good mechanical properties since poor flexibility or strength can produce failure or crack during handling, storage, or use of food products. This work recorded PS values of 8.97–22.30 N (Table 4), higher than some reported in the literature since the acetylation of the starch improved the matrix structure of the EFs. For its part, Maran et al. [7] reported PS values from 5.57 to 13.19 N in EFs based on tapioca starch, and Fitch-Vargas et al. [2] obtained values of 10.39 ± 2.73 N in corn starch-based EFs obtained by a combination of extrusion technology and casting technique.

PS's behavior concerning DS and GC is presented in Fig. 1b. The highest PS values (20.30 ± 0.76 N) were

recorded at low GC (15%) and high DS (0.2). This behavior could be explained by the chemical modification of starch, resulting in more bonds among the EFs' molecules. It has been reported that starch acetyl groups can create more resistant EFs than unmodified starch due to the hydrogen bond interactions among polymeric chains [20]. According to Colussi et al. [10], higher DS increased the tensile strength of acetylated EFs because of the strong intra- and intermolecular interactions. López et al. [6] evaluated the acetylated starch effect with low DS (0.05–0.08) on EFs obtained by extrusion, reporting that the incorporation of modified starch reinforced, despite its low DS, the polymeric matrix increased the tensile strength.

On the other hand, an increase in GC produced a PS decrement (Fig. 1b). This behavior can be attributed to the plasticizer, which can decrease the intermolecular forces of the starch molecule [2]. Furthermore, Chen and Lai [25] found on tapioca starch films that the PS decreased when the GC increased between 25 and 40%.

Carbon dioxide permeability (CO₂P)

The CO₂P mathematical model presented a significant regression model ($P < 0.01$) with $CV = 18.20\%$, $R^2_{adj} = 0.92$, $SD = 1.63 \times 10^{-14}$ mL m Pa⁻¹ s⁻¹ m⁻², and P of $F < 0.01$ (Table 3). The CO₂P was significantly affected mainly by the linear term of DS ($P < 0.01$) with a value of 98.92%, causing higher DS to present lower CO₂P. On the other hand, the CG linear term, although significant, had a lower impact (1.08%); however, its use increased the values of this response variable. The mathematical model is shown in this Eq. (7):

$$CO_2P = -2.43 \times 10^{-13} - 8.47 \times 10^{-12} DS + 9.20 \times 10^{-14} GC \quad (7)$$

In this study, CO₂P from 8.97×10^{-14} to 2.04×10^{-12} mL m Pa⁻¹ s⁻¹ m⁻² was registered (Table 4), being lower values than those obtained by Aguilar-Sánchez et al. [26] in starch-based EFs with nanocomposites and Mexican oregano reported values of 3.14×10^{-13} mL m Pa⁻¹ s⁻¹ m⁻², which showed an adequate structural matrix of the biopolymer. Figure 1c shows the CO₂P's behavior concerning the DS and GC. The CO₂P was found to increase as the GC was increased. This behavior could be attributed to the addition of plasticizers such as glycerol, which reduce intermolecular forces, increase free space in the polymeric matrix, and facilitate CO₂ diffusion through the EFs [6]. On the other hand, as the DS increased, CO₂P decreased because there was an increase in strong intermolecular interactions during acetylation, which reduced the distances between molecules [10]. Chain movement and specific interactions between the functional groups of

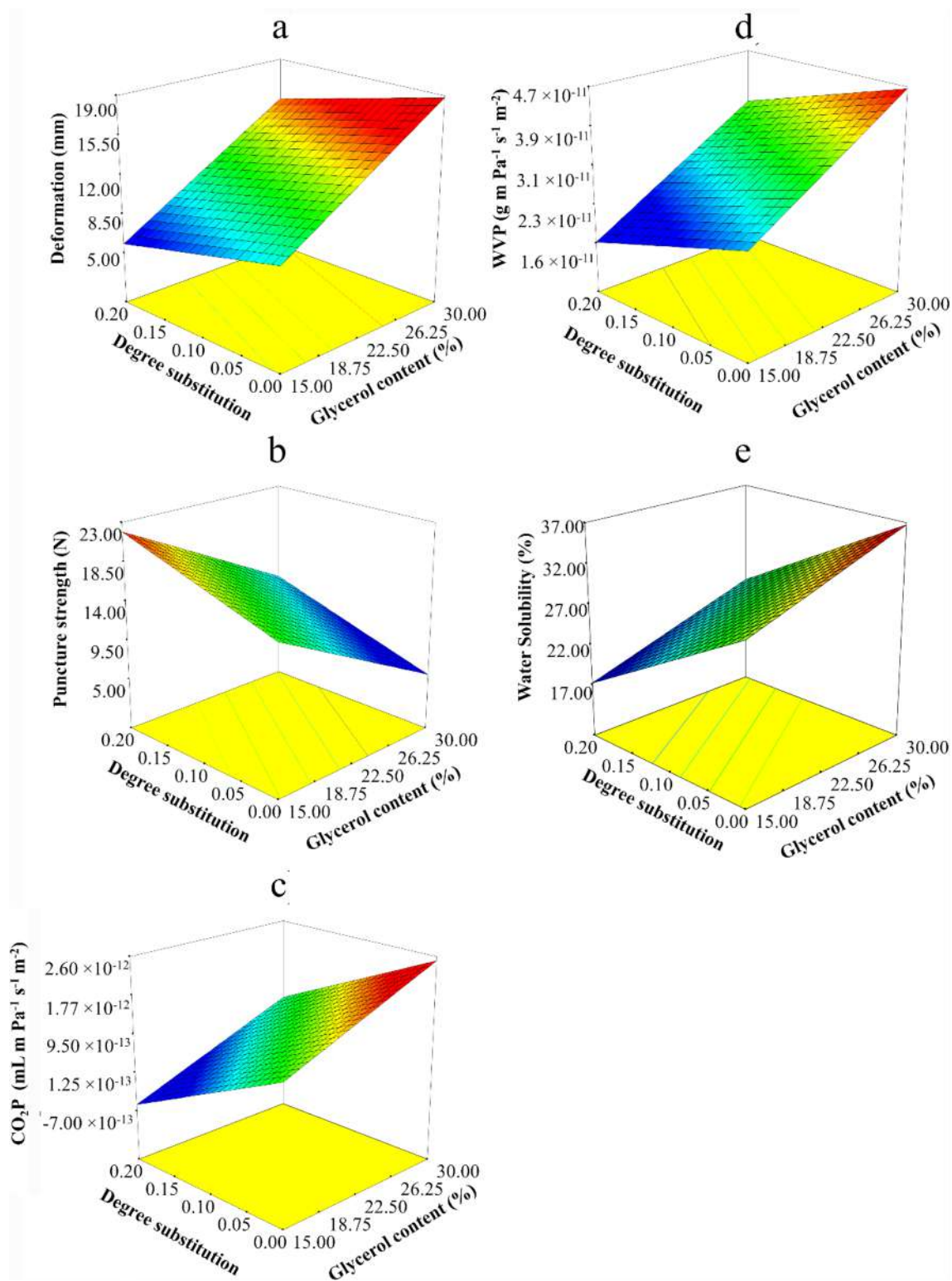


Fig. 1 Response surface plots demonstrating the effects of the interaction between DS and GC on AcEFs response variables. Deformation (a), puncture strength (b), carbon dioxide permeability (c), water vapor permeability (d), water solubility (e)

polymers and the gases determine permeability in amorphous zones, according to García et al. [27]. Similarly, García et al. [28] found that acetylated starch films are less permeable to CO₂ than native ones.

Water vapor permeability (WVP)

A significant regression model was obtained for WVP (Table 3), with values of $R^2_{adj} = 0.82$, $CV = 9.49\%$, $SD = 2.98 \times 10^{-12} \text{ g m Pa}^{-1} \text{ s}^{-1} \text{ m}^{-2}$, and without lack of fit ($P > 0.05$). The linear terms of DS and GC were significant ($P < 0.01$), positively impacting 34.26% and 65.74%, respectively, the increases of both produced a decrease in the WVP values. The mathematical model for WVP is shown in Eq. (8):

$$WVP = +3.15 \times 10^{-11} - 3.69 \times 10^{-12} DS - 7.08 \times 10^{-12} GC \quad (8)$$

Starch-based packaging typically has less effective moisture barriers than synthetic materials [29]. Since the aim of EFs is to limit moisture transfer between the food and the environment, WVP should be as low as possible. In this study, the starch chemical modification by acetylation decreased WVP, recording values from 2.25×10^{-11} to $4.15 \times 10^{-11} \text{ g m Pa}^{-1} \text{ s}^{-1} \text{ m}^{-2}$ (Table 4). These values were lower than those reported in the literature. Saberi et al. [19], for EFs based on pea starch-guar gum, obtained WVP values from 7.39×10^{-10} to $13.87 \times 10^{-10} \text{ g m Pa}^{-1} \text{ s}^{-1} \text{ m}^{-2}$. Likewise, Ghanbarzadeh et al. [30] reported WVP of $6.58 \times 10^{-11} \text{ g m Pa}^{-1} \text{ s}^{-1} \text{ m}^{-2}$ in modified starch/carboxymethyl cellulose-based EFs.

The lowest value of WVP was $2.25 \times 10^{-11} \text{ g m Pa}^{-1} \text{ s}^{-1} \text{ m}^{-2}$, and it was obtained when the DS was higher (0.2) and the GC was lower (15%) (Fig. 1d). It could be due to hydrophobic groups in the acetylated starch. Colussi et al. [10] obtained a lower WVP in acetylated starch films with 0.42 and 0.72 DS than in native starch films. Colivet and Carvalho [9] reported that acetylated cassava starch EFs presented lower WVP values than native cassava starch EFs.

On the other hand, the addition of GC increased the WVP. It is known that the glycerol interactions (hydrogen bonds, ionic, and Van der Waals forces) could increase the intermolecular distances between starch molecules and, therefore, the WVP. Moreover, the hydrophilic character of glycerol promotes water molecule adsorption [7]. According to Motta et al. [18], plasticization promotes the increase of WVP since it favors adsorption and water absorption owing to the enhanced mobility of the polymer chains, which increases the matrix's free space.

Water solubility (S)

According to the statistical analysis, a significant model of regress (P of $F < 0.01$) was found for this response variable (Table 3), with values of $R^2_{adj} = 0.89$, $CV = 5.75\%$, $SD = 1.94\%$ and no lack of fit ($P = 0.86$). The Model F-value of 36.40 implies that the model is significant. There is only a 0.01% chance that a "Model F-value" this large could occur due to noise. The linear terms of DS and GC significantly affected ($P < 0.01$) the S. The linear term of the DS affected 63.94%, decreasing the S values, and the linear term of the GC had an impact of 36.06%, increasing its values.

The mathematical model used is shown in Eq. (9):

$$S = +25.63 - 5.09DS + 2.87GC \quad (9)$$

Figure 1e shows the behavior of S regarding the DS and GC. The S decreased significantly by increasing the DS and decreasing GC; this is positive since high water resistance is required for EFs. The lowest S value ($17.90 \pm 2.52\%$) was obtained at high DS (0.2) and low GC (15%). Table 4 shows the values obtained from the solubility of the edible films of acetylated starch. Colivet and Carvalho [9] found that films made with acetylated cassava starch had greater water resistance than native cassava starch films. Pérez-Gallardo et al. [31] and Ghanbarzadeh et al. [32] reported that acetylated starch showed low solubility due to increased interactions among carboxyl groups of acetylated starch and hydroxyl groups. Also, some researchers have investigated the plasticizer effect on the S [2, 33]. According to Matta Jr et al. [34], the hydrophilic behavior of glycerol significantly impacts the S of starch-based EFs since glycerol can interact with the polymeric matrix, increasing space between the chains and facilitating the diffusion of water and increasing the S.

Numerical optimization

Numerical optimization was employed to find the best treatment of DS (0–0.2) and GC (15–30%) and obtain EFs with high D and PS values and low CO₂P, WVP, and S values. According to the optimization for AcEFs, the best conditions were DS = 0.16 and GC = 18.30%. Through the optimum conditions, the following predicted values were obtained for each of the mathematical models of the response variables: $D = 8.54 \pm 1.04 \text{ mm}$, $PS = 18.49 \pm 1.68 \text{ N}$, $CO_2P = 9.38 \times 10^{-14} \pm 1.63 \times 10^{-14} \text{ mL m Pa}^{-1} \text{ s}^{-1} \text{ m}^{-2}$, $WVP = 2.26 \times 10^{-11} \pm 2.98 \times 10^{-12} \text{ g m Pa}^{-1} \text{ s}^{-1} \text{ m}^{-2}$, and $S = 23 \pm 1.94\%$. The bar graph of individual and global desirability of the response variables of

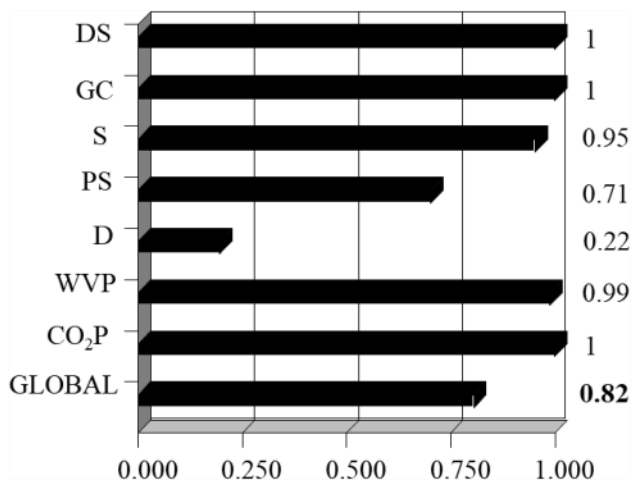


Fig. 2 Individual and global desirability of the process variables and responses analyzed during the optimization of AcEFs

the AcEFs is shown in Fig. 2. The highest desirability is 1, and the lowest desirability is 0. The desirability value indicates the probability of obtaining significantly similar results ($P > 0.05$) for an optimal model. The individual desirability of each response variable generated overall global desirability of 0.82. This result shows that the optimal model predicted by the software is validated.

AcEFs were elaborated and characterized by employing the optimum conditions to verify the values predicted by the model. The average values and standard deviations obtained from the response variables of the optimal treatment of AcEFs are shown below: $D = 8.87 \pm 1.90$ mm, $PS = 19.09 \text{ N} \pm 2.34$, $CO_2P = 8.17 \times 10^{-14} \pm 6.50 \times 10^{-14} \text{ mL m Pa}^{-1} \text{ s}^{-1} \text{ m}^{-2}$, $WVP = 2.01 \times 10^{-11} \pm 3.58 \times 10^{-12} \text{ g m Pa}^{-1} \text{ s}^{-1} \text{ m}^{-2}$, and $S = 22.40 \pm 2.12\%$. There were no significant differences between the predicted values of the mathematical models and the experimental values of the optimal treatment ($P > 0.05$). This result demonstrated that the models developed were suitable.

X-ray diffraction (XRD)

Absorption peaks and an amorphous zone characterize X-ray diffraction (XRD) patterns of starch EFs; as the amorphous zone grows, the crystallinity of the sample decreases [27]. The XRD patterns of native starch, acetylated modified corn starch, and AcEFs are shown in Fig. 3. Native starch recorded an A-type crystallinity XRD pattern, representative of cereal starch, with pronounced peaks at values 2θ of $\approx 18.8^\circ$ and $\approx 24^\circ$. The XRD reflection intensity of the acetylated modified corn starch was lower than native starch. The formation of these structures could be caused by the interaction of starch molecules, particularly amylose chains,

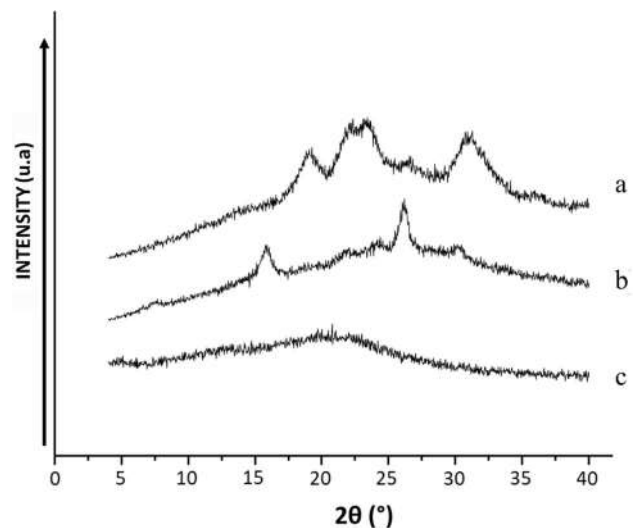


Fig. 3 XRD patterns of native starch (a), acetylated modified starch (b), and AcEFs (c)

with the acetyl ester. The modified corn starch showed a combination of type A and Vh crystallinity patterns, indicating that modified corn starch was not completely degraded. The Vh-type pattern occurs during thermoplastic starch processing due to the formation of complexes between amylose and glycerol and records 2θ angles at approximately 7° , 13° , 20° , and 23° [35]. However, some diffraction peaks with type A pattern characteristics were found, suggesting that the material is not wholly disintegrated [13]. The AcEFs showed lower intensity peaks than the modified corn starch (Fig. 3). This behavior is similar to Fitch-Vargas et al. [2] since when thermoplastic starch was processed under extreme conditions, the original structure was drastically modified, resulting in an X-ray diffractogram with amorphous zones or new diffraction peaks corresponding to new structures.

Moreover, the native starch showed a higher crystallinity than AcEFs and acetylated modified corn starch. According to Pérez Gallardo et al. [31], the starch crystallinity results from the linear amylose content (compared to amylopectin, which is highly branched). The relative crystallinity (RC) was $16.14 \pm 1.4\%$ for native starch and decreased to $6.20 \pm 1.02\%$ for acetylated modified corn starch. These results indicate that reactive extrusion modification partially destroyed the native starch crystalline structure [2]. Similarly, Zhang et al. [36] found that acetic acid changes the crystalline structure of yellow ginger-modified starch by replacing certain hydroxyl groups with acetyl groups, limiting the formation of inter- and intramolecular hydrogen bonds. The RC for AcEFs was $4.27 \pm 0.4\%$. The starch molecular order is disrupted during the thermal treatment of casting, according to Gutiérrez et al. [37], resulting in an amorphous structure. As a result, the AcEFs showed an amorphous phase with a small crystalline portion. El Halal

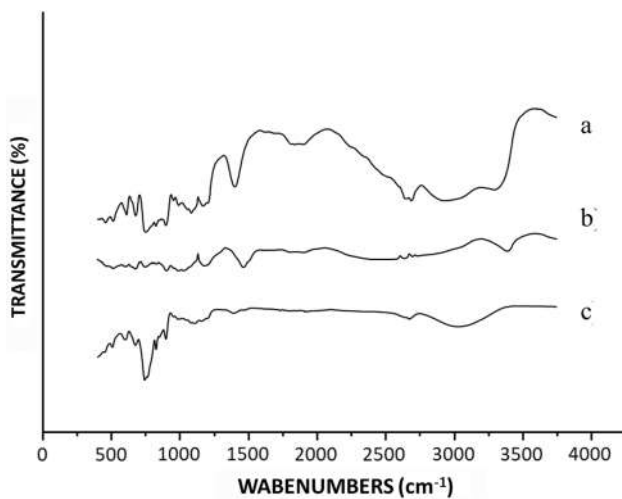


Fig. 4 FT-IR spectra of native starch (a); acetylated modified starch (b); and AcEFs (c)

et al. [20] reported that acetylated starch films had lower RC than native starch films, owing to reduced intramolecular and intermolecular hydrogen bonding in the esterification process, which resulted in lower RC.

Infrared spectroscopy analysis (FT-IR)

FT-IR analysis detected likely molecular interactions and functional groups in acetylated starch and AcEFs. Figure 4 shows the FT-IR spectra of native starch, acetylated modified corn starch, and AcEFs. Peaks at 1002 and 1356 cm^{-1} in the FT-IR spectrum of native starch corresponded to C–O bond stretching [13]. The absorption peaks at approximately 1664, 3196, and 2072 cm^{-1} correspond to the water molecule, OH-group vibration, and C–H vibration stretch [38].

The acetylated modified corn starch lowered the peaks' intensity (Fig. 4b), possibly due to chemical bonding breaking during the extrusion process. New absorption peaks at 1732 and 1134 cm^{-1} were ascribed to the carbonyl C=O and C–O stretching vibrations.

These new absorption bands show the ester carbonyl groups produced during the chemical changes of native starch [9, 13]. Peaks at 3242–3641 cm^{-1} were found in the acetylated modified corn starch, associated with the O–H groups of water and glucose molecules [38, 39]. Differences in the bands' displacement and intensity were detected in the AcEFs' FT-IR spectra (Fig. 4c), probably due to new interactions among the EFs' constituents [20]. Also, AcEFs recorded a spectrum with peaks at 1512 cm^{-1} . These peaks are related to the functional groups of the reagent used during the chemical modification of starch by acetylation. These findings suggest that adding acetyl groups to starch

can impact intramolecular interactions, hydrogen bonding integrity, and the film matrix's stability [40].

Conclusion

The mathematical models of the response variables showed a good fit to find the best conditions of DS and GC and obtain AcEFs with adequate barrier and mechanical properties. The numerical optimization helped find the optimum blend to produce EFs with good mechanical characteristics and low S, WVP, and CO_2P . The microstructural analysis (XRD and FT-IR) demonstrated the effect of reactive extrusion on the starch chemical modification and new hydrogen bonding interactions at AcEFs. As a result, AcEFs could be employed to enhance food products' water and carbon dioxide permeability, improving their storage life.

Acknowledgements Not applicable.

Author contributions EA-P: Designed the experiment, interpreted the results, and prepared the manuscript. AC-C: Led all the experiments and analyzed the data. PRF-V, LFP-V, ILC-H, and JJZ-M: Contributed technical assistance and helped to revise the manuscript. AC-C: Oversaw the whole research in general and organized the manuscript.

Funding This study did not receive specific funding from public agencies or commercial or not-for-profit sectors.

Declarations

Conflict of interest The manuscript is an original work and is not being considered for publication in other media with substantial circulation. All previously published works cited in the manuscript have been fully acknowledged. All authors have contributed substantially to the manuscript and approved the final submission. No conflicts of interest exist between the authors and the reviewers who proposed to evaluate this manuscript. This manuscript was prepared strictly according to the journal format as provided in the instruction to the authors.

References

1. G. Ghoshal, H.J. Chopra, *Food Meas. Charact.* **16**(2), 1274–1290 (2022). <https://doi.org/10.1007/s11694-021-01234-9>
2. P.R. Fitch-Vargas, E. Aguilar-Palazuelos, J.J. Zazueta-Morales, M.O. Vega-García, J.E. Valdez-Morales, F. Martínez-Bustos, N. Jacobo-Valenzuela, *Food Sci.* **81**(9), E2224–E2232 (2016). <https://doi.org/10.1111/1750-3841.13416>
3. L. Han, Y. Qin, D. Liu, H. Chen, H. Li, M. Yuan, *Innov. Food Sci. Emerg. Technol.* **29**, 288–294 (2015). <https://doi.org/10.1016/j.ifset.2015.04.008>
4. M. Yıldırım-Yalçın, H. Sadıkoğlu, M.J. Şeker, *J. Food Meas. Charact.* **15**(5), 4669–4678 (2021). <https://doi.org/10.1007/s11694-021-01038-x>
5. T.J. Gutiérrez, N.J. Morales, E. Pérez, M.S. Tapia, L. Famá, *Food Package Shelf Life* **3**, 1–8 (2015). <https://doi.org/10.1016/j.fpsl.2014.09.002>

6. O.V. López, N.E. Zaritzky, M.V.E. Grossmann, M.A. García, J. Food Eng. **116**(2), 286–297 (2013). <https://doi.org/10.1016/j.jfoodeng.2012.12.032>
7. J.P. Maran, V. Sivakumar, R. Sridhar, V.P. Immanuel, Ind. Crop Prod. **42**, 159–168 (2013). <https://doi.org/10.1016/j.indcrop.2012.05.011>
8. S.M. Beyan, T.A. Amibo, V.P.J. Sundramurthy, J. Food Meas. Charact. **16**(3), 2259–2272 (2022). <https://doi.org/10.1007/s11694-022-01338-w>
9. J. Colivet, R.A. Carvalho, Ind. Crop Prod. **95**, 599–607 (2017). <https://doi.org/10.1016/j.indcrop.2016.11.018>
10. R. Colussi, V.Z. Pinto, S.L.M. El Halal, B. Biduski, L. Prietto, D.D. Castilhos, A.R.G. Dias, Food Chem. **221**, 1614–1620 (2017). <https://doi.org/10.1016/j.foodchem.2016.10.12>
11. X. Wu, P. Liu, P.L. Ren, J. Tong, J. Zhou, Starch-Stärke **66**(5–6), 508–514 (2013). <https://doi.org/10.1002/star.201300194>
12. N. Hu, L.J. Li, Food Process. Preserv. (2021). <https://doi.org/10.1111/jfpp.15431>
13. C.I.K. Diop, H.L. Li, B.J. Xie, J. Shi, Food Chem. **126**(4), 1662–1669 (2011). <https://doi.org/10.1016/j.foodchem.2010.12.05>
14. C.I. La Fuente, L. do Val Siqueira, P.E.D. Augusto, C.C. Tadini, Innov. Food Sci. Emerg. Technol. **75**, 102906 (2022). <https://doi.org/10.1016/j.ifset.2021.102906>
15. B. Murúa-Pagola, C.I. Beristain-Guevara, F. Martínez-Bustos, J. Food Eng. **91**(3), 380–386 (2009). <https://doi.org/10.1016/j.jfoodeng.2008.09.03>
16. A. Calderón-Castro, N. Jacobo-Valenzuela, L.A. Félix-Salazar, J.J. Zazueta-Morales, F. Martínez-Bustos, P.R. Fitch-Vargas, E. Aguilar-Palazuelos, J. Food Sci. Technol. (2019). <https://doi.org/10.1007/s13197-019-03863-x>
17. S. Yao, B.J. Wang, Y.M. Weng, Food Package Shelf Life **32**, 100845 (2022). <https://doi.org/10.1016/j.fpsl.2022.100845>
18. J.F.G. Motta, A.R. de Souza, S.M. Gonçalves, D.K.S.F. Madella, C.W.P. de Carvalho, L. Vitorazi, N.R. de Melo, Food Bioprocess. Technol. **13**(12), 2082–2093 (2020). <https://doi.org/10.1007/s11947-020-02548-0>
19. B. Saberi, Q.V. Vuong, S. Chockchaisawasdee, J.B. Golding, C.J. Scarlett, C.E. Stathopoulos, Food Bioprocess. Technol. **10**(12), 2240–2250 (2017). <https://doi.org/10.1016/j.jbiomac.2017.06.051>
20. S.L.M. El Halal, R. Colussi, B. Biduski, J.A. Evangelho, G.P. Bruni, M.D. Antunes, E. Zavareze, J. Sci. Food Agric. **97**(2), 411–419 (2016). <https://doi.org/10.1002/jsfa.7773>
21. E. Ayranci, S. Tunc, Food Chem. **72**(2), 231–236 (2001). [https://doi.org/10.1016/s0308-8146\(00\)00227-2](https://doi.org/10.1016/s0308-8146(00)00227-2)
22. M. Chiumarelli, M.D. Hubinger, Food Hydrocoll. **38**, 20–27 (2014). <https://doi.org/10.1016/j.foodhyd.2013.11.013>
23. S. Mali, M.V.E. Grossmann, M.A. García, M.N. Martino, N.E. Zaritzky, Food Hydrocoll. **19**(1), 157–164 (2005). <https://doi.org/10.1016/j.foodhyd.2004.05.002>
24. M.A. Cerqueira, B.W. Souza, J.A. Teixeira, A.A. Vicente, Food Bioprocess. Technol. **6**(6), 1600–1608 (2013). <https://doi.org/10.1007/s11947-011-0753-x>
25. C.H. Chen, L.S. Lai, Food Hydrocoll. **22**(8), 1584–1595 (2008). <https://doi.org/10.1016/j.foodhyd.2007.11.006>
26. R. Aguilar-Sánchez, R. Munguía-Pérez, F. Reyes-Jurado, A.R. Navarro-Cruz, T.S. Cid-Pérez, P. Hernández-Carranza, R. Avila-Sosa, Molecules. **24**(12), 2340 (2019). <https://doi.org/10.3390/molecules24122340>
27. M.A. García, M.N. Martino, N.E. Zaritzky, Starch-Stärke **52**(4), 118–124 (2000). [https://doi.org/10.1002/1521-379X\(200006\)52:4<118::AID-STAR118>3.0.CO;2-0](https://doi.org/10.1002/1521-379X(200006)52:4<118::AID-STAR118>3.0.CO;2-0)
28. M.P.M. García., M.C. Gómez-Guillén, M.E. López-Caballero, G.V. Barbosa-Cánovas, (CRC Press, Boca Raton, Florida, 2016), pp. 616
29. M.A. Sani, M. Azizi-Lalabadi, M. Tavassoli, K. Mohammadi, D.J. McClements, Nanomaterials **11**(5), 1331 (2021). <https://doi.org/10.3390/nano11051331>
30. B. Ghanbarzadeh, H. Almasi, A.A. Entezami, Innov. Food Sci. Emerg. Technol. **11**(4), 697–702 (2010). <https://doi.org/10.1016/j.ifset.2010.06.001>
31. A. Pérez-Gallardo, L.A. Bello-Pérez, B. García-Almendárez, G. Montejano-Gaitán, G. Barbosa-Cánovas, C. Regalado, Starch-Stärke **64**(1), 27–36 (2011). <https://doi.org/10.1002/star.201100042>
32. B. Ghanbarzadeh, H. Almasi, A.A. Entezami, Ind. Crop Prod. **33**(1), 229–235 (2011). <https://doi.org/10.1016/j.indcrop.2010.10.016>
33. R. Sothornvit, P. Rodsamran, Postharvest Bio. Technol. **47**(3), 407–415 (2008). <https://doi.org/10.1016/j.postharvbio.2007.08>
34. M.D. Matta Jr., S.B.S. Sarmiento, C.I.G.L. Sarantópoulos, S.S. Zocchi, Polímeros. **21**(1), 67–72 (2011). <https://doi.org/10.1590/s0104-14282011005000011>
35. J.F. Mendes, L.B. Norcino, H.H.A. Martins, A. Manrich, C.G. Otoni, E.E.N. Carvalho, L. Mattoso, Food Hydrocoll. **100**, 105428 (2020). <https://doi.org/10.1016/j.foodhyd.2019.105428>
36. L. Zhang, W. Xie, X. Zhao, Y. Liu, W. Gao, Thermochim. Acta **495**(1–2), 57–62 (2009). <https://doi.org/10.1016/j.tca.2009.05.019>
37. T.J. Gutiérrez, J. Suniaga, A. Monsalve, N.L. García, Food Hydrocoll. **54**, 234–244 (2016). <https://doi.org/10.1016/j.foodhyd.2015.10.012>
38. F. Cruces, M.G. García, N.A. Ochoa, Food Bioprocess. Technol. (2021). <https://doi.org/10.1007/s11947-021-02628-9>
39. H.Y. Kim, J. Jane, B. Lamsal, Ind. Crop. Prod. **95**, 175–183 (2017). <https://doi.org/10.1016/j.indcrop.2016.10.025>
40. J. Li, F. Ye, J. Liu, G. Zhao, Food Hydrocoll. **46**, 226–232 (2015). <https://doi.org/10.1016/j.foodhyd.2014.12.017>

Publisher's Note Springer Nature remains neutral with regard to jurisdictional claims in published maps and institutional affiliations.

Springer Nature or its licensor (e.g. a society or other partner) holds exclusive rights to this article under a publishing agreement with the author(s) or other rightsholder(s); author self-archiving of the accepted manuscript version of this article is solely governed by the terms of such publishing agreement and applicable law.